Available online at www.sciencedirect.com
ScienceDirect
Polymer 48 (2007) 2874–2881
polymer
www.elsevier.com/locate/polymer

Robust polymer gel opals – An easy approach by inter-sphere cross-linking gel nanoparticle assembly in acetone

Bo Zhou [a,b,1], Jun Gao [a,b,2], Zhibing Hu [a,b,*]

[a] Department of Physics, University of North Texas, P.O. Box 311497, Denton, TX 76203, United States
[b] Department of Material Science and Engineering, University of North Texas, P.O. Box 311497, Denton, TX 76203, United States

Received 5 February 2007; received in revised form 28 February 2007; accepted 3 March 2007
Available online 14 March 2007

Abstract

Narrowly distributed poly(*N*-isopropylacrylamide-*co*-acrylic acid) (PNIPAM-*co*-AA) nanoparticles with different particle sizes were synthesized and used as building blocks to form crystalline polymer gels. It was found that PNIPAM-*co*-AA nanoparticles can self-assemble into crystalline arrays in organic solvent as indicated by their iridescent colors and by the scattering peak in UV–vis spectra caused by Bragg diffraction. These crystalline structures were stabilized in acetone using epichlorohydrin to cross-link neighboring particles at ~90 °C. The resultant opals had much higher polymer concentration than that of similar hydrogels. Due to their higher polymer contents, these opals had much better mechanical strength and could undergo the solvent exchange from an organic solvent to water without being broken. Kinetics of the solvent exchange was measured and explained in terms of the volume phase transition of the PNIPAM in mixed solvents. Shear modulus of the opal was measured in the linear stress-yield ranges for the same gel crystals in both acetone and water.

Keywords: Polymer gels; Opal; Nanoparticles

1. Introduction

Polymer gels have been studied extensively as biomaterials [1,2], carriers for controlled drug release [3,4], artificial muscles [5,6] and switches [7]. As the newest emerging branch in the polymer gels research, photonic polymer gels are gaining an increased attention due to their unique optical properties arising from their periodic structures [8–18]. Some applications in narrow band optical rejection filters [8,9], nanosecond nonlinear optical switching and limiting devices [10] and sensors [11–18] have already been performed. Most current studies focus on the manufacture and the use of nanostructured polymer gels in aqueous suspensions.

The mechanical strength of the bonded particle assembly in water was usually weak [11]. This is because the crystallization of a hard sphere system can take place at the volume fraction around 0.5 at which the particles only slightly contact with each other [19]. As a result, the number of effective cross-link points between neighboring particles are not many. Recently, it was found that PNIPAM microgels can form crystals at an elevated temperature [14b]. This dispersion was then cooled down to room temperature, resulting in the expansion of PNIPAM nanoparticles. The expansion increased the contact interfaces between neighboring particles and resulted in the increase of the number of effective cross-link points subsequently [20].

Here we propose and demonstrate an approach to form high polymer concentration crystalline gels. The central idea is to first self-assemble monodisperse nanoparticles into a crystalline structure in organic solvent at room temperature, then raise the temperature of the nanoparticle organic dispersion. At this elevated temperature, the gel nanoparticles tend to swell more.

* Corresponding author. Department of Physics, University of North Texas, P.O. Box 311497, Denton, TX 76203, United States. Tel.: +1 940 565 4583; fax: +1 940 565 2515.
E-mail address: zbhu@unt.edu (Z. Hu).
[1] Present address: 7912 Elk Mountain TRL, McKinney, TX 75070, United States.
[2] Present address: enGene Inc., 2386 East Mall, Vancouver, BC V6T 1Z3, Canada.

0032-3861/$ - see front matter © 2007 Elsevier Ltd. All rights reserved.
doi:10.1016/j.polymer.2007.03.025

The expansion of the gel nanoparticles can not only lock the crystalline structure formed at room temperature but also enhance the contact interface between neighboring particles. After covalently bonding neighbor particles at this elevated temperature, the crystalline structure can be permanently stabilized. Indeed, this approach can lead to strong gels with crystalline structures.

In this study, we first synthesized poly(*N*-isopropylacrylamide-*co*-acrylic acid) (PNIPAM-*co*-AA) gel nanoparticles using precipitation polymerization method [21], then dispersed the particles in acetone containing epichlorohydrin and allowed them to self-assemble into crystalline arrays at a suitable polymer concentration. The crystalline structure was temporarily stabilized upon heating the dispersions to ~90 °C, and permanently set via inter-particle chemical reaction. The gel properties including particle sizes, the angular dependence of the colors and kinetics of solvent exchange were characterized using light scattering, UV-vis spectroscopy, and mechanical testing, respectively.

2. Experimental section

2.1. Preparation of nanoparticles

The PNIPAM-*co*-AA nanoparticles were prepared in a 500 ml reactor under a nitrogen atmosphere with gentle stirring. *N*-Isopropylacrylamide (NIPAM; 3.80 g), *N*,*N*′-methylenebisacrylamide (BIS; 0.066 g), acrylic acid (AA; 0.11 g) and a certain amount of sodium dodecyl sulfate (SDS) were dissolved in 234 ml deionized water in the reactor. The reactor was incubated in a water bath and heated to 70 °C. The solution was stirred for 30 min with a nitrogen purge to remove oxygen. Potassium persulfate (KPS; 16.6 g, 1 wt%) was then added to start the reaction. The reaction was carried out at 70 °C for 4 h.

2.2. Fabrication of crystalline PNIPAM-co-AA nanoparticle networks

At room temperature, acetone was added to the resultant water dispersion to precipitate PNIPAM-*co*-AA nanoparticles. The precipitates were washed with acetone–water mixtures and dried before being re-dispersed in acetone to an aimed polymer concentration. Epichlorohydrin (ECh) (5 wt% of the dispersion) was added for inter-sphere cross-linking. The concentrated dispersions were vortexed followed by centrifuging to eliminate inhomogeneity. Crystalline structures formed after the dispersion stood for several hours depending on concentration. The chemical cross-linking was conducted by incubating the sealed colloidal crystal dispersions in acetone at ~90 °C for 6 h. Specifically, the dispersion of nanoparticles (1–2 ml) was placed into a small capped vial for colloidal crystals to grow at room temperature. Then the vial was incubated in a 90 °C oven with its cap sealed after reaching ~90 °C. A bigger vial was used to hold the small one for safety control. Under increased pressure in a gel matrix, the boiling temperature of acetone was far above 56.3 °C, the boiling point of pure acetone. We did not observe any boiling or turbulence under the experimental conditions.

2.3. Characterizations

The particle size was characterized by dynamic light scattering method. A laser light scattering (LLS) spectrometer (ALV, Germany) equipped with an ALV-5000 digital time correlator was used with a helium–neon laser (Uniphase 1145P, output power of 22 mW and wavelength of 632.8 nm) as the light source. The incident light was vertically polarized with respect to the scattering plane and the light intensity was set with a beam attenuator (Newport M-925B). The scattered light was conducted through an optical fiber leading to an active quenched avalanche photo diode (APD), which serves as the detector. The coherent factor β in dynamic laser light scattering was about 0.98. The fluctuation of the scattered intensity with time t, $g^{(1)}(q,t)$, is the first-order electric field time correlation function $E(t,q)$ and is related to the line-width distribution $G(\Gamma)$ by [22,23]

$$g^{(1)}(t,q) = \langle E(t,q)E^*(0,q)\rangle = \int_0^\infty G(\Gamma)\,\mathrm{e}^{-\Gamma t}\,\mathrm{d}\Gamma \tag{1}$$

where $G(\Gamma)$ can be obtained from the Laplace inversion of $g^{(1)}(q,t)$. $g^{(1)}(q,t)$ was analyzed by a cumulant analysis to obtain the average line width $\langle\Gamma\rangle$ and the polydispersity index (PDI $= 1 + \mu_2/\langle\Gamma\rangle^2$, where $\mu_2 = \int_0^\infty G(\Gamma)(\Gamma - \langle\Gamma\rangle)^2\mathrm{d}\Gamma$). The extrapolation of Γ/q^2 to $q \to 0$ led to the translational diffusion coefficient (D). The corresponding analysis of this function yields the diffusion coefficient D, which can be translated into the hydrodynamic radius R_h by the Stokes–Einstein relation: $\langle R_\mathrm{h}\rangle = k_\mathrm{B}T/(6\pi\eta D)$, where k_B, T, and η are the Boltzmann constant, the absolute temperature, and the solvent viscosity, respectively. The dynamic light scattering experiments were performed at the scattering angle $\theta = 90°$.

The turbidity of the PNIPAM-*co*-AA nanoparticle dispersions as a function of the wavelength was measured using a UV–vis spectrophotometer (Agilent 8453).

The shear modulus of the resulted PNIPAM-*co*-AA gels was measured using a digital force gauge (Shimpo, Japan). The shear modulus was determined by uniaxially compressing a cylindrical gel with a glass plate. The height and radius are measured using a caliber with an accuracy of 0.05 mm. The force applied to the plate was measured with the gauge pre-calibrated. For each applied force F, the length of the gel sample was recorded.

3. Results and discussion

3.1. PNIPAM-co-AA nanoparticles

PNIPAM-*co*-AA nanoparticles were synthesized using precipitation polymerization as shown in Scheme 1(a) [21]. The particle sizes were controlled by varying the amounts of surfactant SDS used in the syntheses (Table 1). The hydrodynamic radius distributions of PNIPAM-*co*-AA particles in water at various synthesis surfactant concentrations are shown in Fig. 1(i). A very narrow particle size distribution (PDI < 1.05)

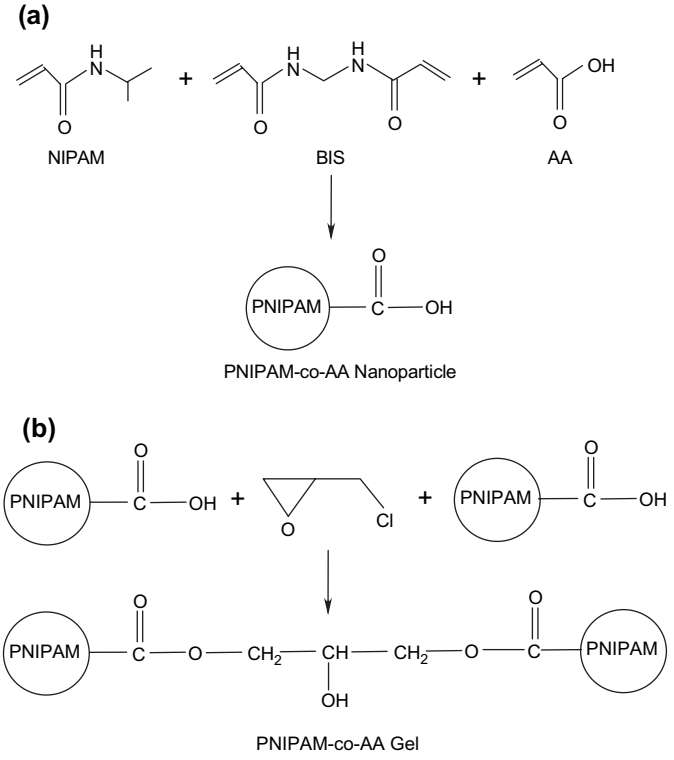

Scheme 1.

contributes to the formation of PNIPAM-*co*-AA colloidal crystals.

The particles were then precipitated by adding acetone to PNIPAM-*co*-AA water dispersion, purified by washing with mixed solvents and eventually transferred into acetone. Based on the study of the collapse of polymer gels by Tanaka [24,25], acetone can act as a good sedimentary agent in the colloidal suspensions at certain acetone–water ratio under room temperature. Although pure acetone is a good solvent for PNIPAM-*co*-AA nanoparticles, a mixture of water–acetone can be a co-nonsolvent depending on the mixture composition. Fig. 1(ii) shows the different degrees of swelling of PNIPAM-*co*-AA particles by comparing the hydrodynamic radius distributions of these particles in acetone and in water, respectively. One can see that the particle size of PNIPAM-*co*-AA is smaller in acetone than that in water, consisting with a previous report [26]. The lower degree of swelling of PNIPAM-*co*-AA gel spheres in acetone than in water enabled us to fabricate crystalline gels with much higher solid contents at the effective volume fraction suitable for the crystalline formation [19].

3.2. Self-assembling and stabilization of PNIPAM-co-AA nanoparticles in acetone

At the solid content of 10 wt% in acetone–ECh, nanoparticles can self-assemble into colloidal crystals. The crystals are easy to observe due to their iridescent patterns. The self-assembled crystalline structure can be better revealed by UV–vis spectroscopy as shown in Fig. 2 for samples of batches 1, 2 and 3 with various particle sizes. Here all dispersions contain polymer content of 10 wt%. The UV–vis spectra exhibit either a sharp peak (Batch III) or a shoulder-like peak (Batch I) or a shoulder where the absolute slope increases sharply (Batch II). A sharp peak indicates a long-ranged order structure, while the shoulder-like shape in the spectra shows a short-ranged, less well-organized order [27], all of which correspond to the color of the gels. Fig. 2 also gives that the peak/shoulder position shifts to a short wavelength as the particle size decreases. The turbidity peaks originate from Bragg diffraction. Constructive interference occurs if Bragg condition of $2nd\sin\theta = m\lambda$ is satisfied, where d, θ, n, λ and m are the lattice spacing, diffraction angle, refractive index of the gel medium, wavelength of light in vacuum and diffraction order, respectively. The decrease in particle size of nanoparticle spheres reduces the inter-particle distance d so that λ_c shifts to a lower wavelength [27].

For crystalline nanoparticle networks formation, crystals were formed in acetone at the solid content of ~10 wt%, much higher than ~3 wt% that is required for the formation of crystals in water [27]. The crystalline structures of nanoparticles in acetone have been stabilized based on cross-linking reaction mechanism [11] as shown in Scheme 1(b). The carboxyl groups on the surface of nanospheres are cross-linked in acetone by ECh at ~90 °C to form three-dimensional nanoparticle network. This method has two advantages over intersphere cross-linking in water. First, the crystalline nanoparticle network forms at a much higher polymer concentration due to the lower swelling ability of the precursor nanospheres in acetone. Second, at an increased temperature (90 °C) for intersphere cross-linking, acetone may become a better solvent for PNIPAM-AA particles. This results in excessive swelling of the PNIAPM nanoparticles that squeeze against each other in a confined space. As a result, the particles are more closely

Table 1
Synthesis conditions of PNIPAM-*co*-AA nanoparticles

	Batch						
	I	II	III	IV	V	VI	VII
NIPAM (g)	3.80	3.80	3.80	3.80	3.80	3.80	3.80
BIS (g)	0.066	0.066	0.066	0.066	0.066	0.066	0.066
SDS (g)	0.228	0.208	0.155	0.123	0.102	0.063	0
AA (g)	0.11	0.11	0.11	0.11	0.11	0.11	0.11
KPS (mg)	166	166	166	166	166	166	166
R_h (nm)	122	161	213	295	360	524	720

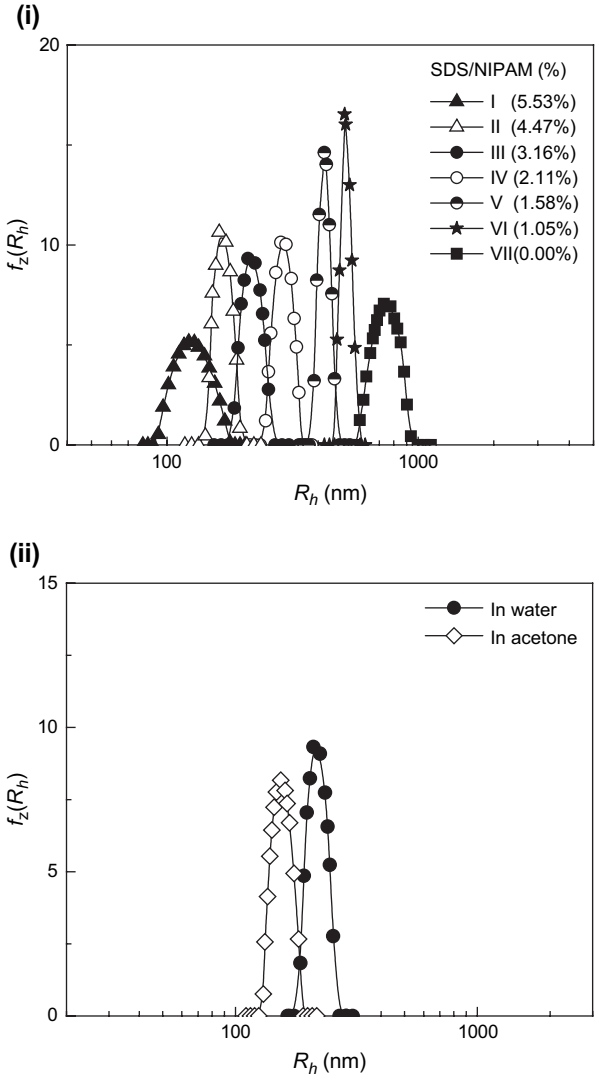

Fig. 1. (i) Hydrodynamic radius distributions $f(R_h)$ of the precursor PNIPAM-*co*-AA gel nanoparticles at 25 °C in water (Batches I–VII) from left to right were synthesized using different weight ratio of surfactant SDS to NIPAM. (ii) Particle size distributions of the PNIPAM-*co*-AA gel nanoparticles (Batch III) at 25 °C in water ($\langle R_h \rangle = 213$ nm) and in acetone ($\langle R_h \rangle = 142$ nm).

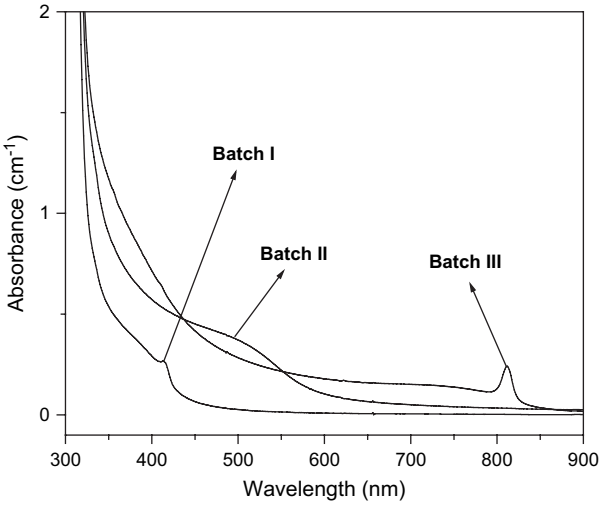

Fig. 2. UV–vis absorbance spectra of the PNIPAM-*co*-AA nanoparticles in acetone at 10% polymer concentration from particles prepared in Batch I (122 nm), Batch II (161 nm), and Batch III (213 nm). The particle sizes were measured in water at room temperature using dynamic light scattering method.

packed at 90 °C than at room temperature. The competitive swelling of the nanoparticles not only stabilizes the periodic crystalline structure but also enhances the efficiency of chemical inter-sphere cross-linking at ~90 °C. As a result, shear modulus of the acetone nanoparticle network is much higher, as will be presented later.

3.3. Properties of stabilized self-assembled nanoparticles

PNIPAM-*co*-AA gel nanoparticles with different sizes can form gel nanoparticle networks with different colors, as shown in Fig. 3(i). The smaller precursor size corresponds to a color with a shorter wavelength due to Bragg diffraction. Crystalline PNIPAM-*co*-AA gel is formed from the precursor particles (Batch III) with $\langle R_h \rangle$ of 213 nm in a fully swollen state. The picture was taken after transferring gel nanoparticle networks (by injecting acetone into the bottom of the original vials to push the gels out) into bigger vials containing acetone and then washing for a few days until an equilibrium state was reached. Crystalline PNIPAM-*co*-AA gels can diffract visible light due to their suitable inter-sphere distance and the slight difference in refractive indices between PNIPAM-*co*-AA nanoparticles and interstitial environment.

Fig. 3(ii) shows the Bragg diffraction of crystalline PNIPAM-*co*-AA gel (Batch III) suspended in ECh. In the experiment as shown in Fig. 3(ii), after passing through a cylindrical lens, a thin sheet of white light shined on this colloidal crystalline gel that was placed in a vial with a diameter of 2 cm. As the scattering angle (φ) with respect to the direction of incident beam decreases from 165° to 85°, the color of the dispersion changes from red to blue. Here the scattering angle equals to twice of the diffraction angle (θ). At the fixed values of d and m, as the scattering angle increases, the wavelength becomes longer (or the color is shifted from blue to red) as observed.

The solvent exchange from acetone to water was performed. Pictures were taken at different stages and shrinking–swelling kinetics was recorded as the function of time. Crystals can be observed clearly from an acetone soaked crystalline gel (Fig. 4(i)-a). After immersing the gel into large amount of water, water–acetone exchange started rapidly. The gel became turbid and shrank into a smaller size in a few minutes (Fig. 4(i)-b). This process was slowed down and the gel reached its smallest size in about 60 min (a kinetics curve in Fig. 4(ii)). After that, the surface of the gel began to swell, resulting in a colored shell (Fig. 4(i)-c). The swelling continued and the gel restored its crystalline state in water (Fig. 4(i)-d). Note the dimension of the gel increased by ~30% after the solvent exchange and the color of crystal changed from shorter (green in Fig. 4(i)-a) to longer (pink in Fig. 4(i)-d) wavelength accordingly.

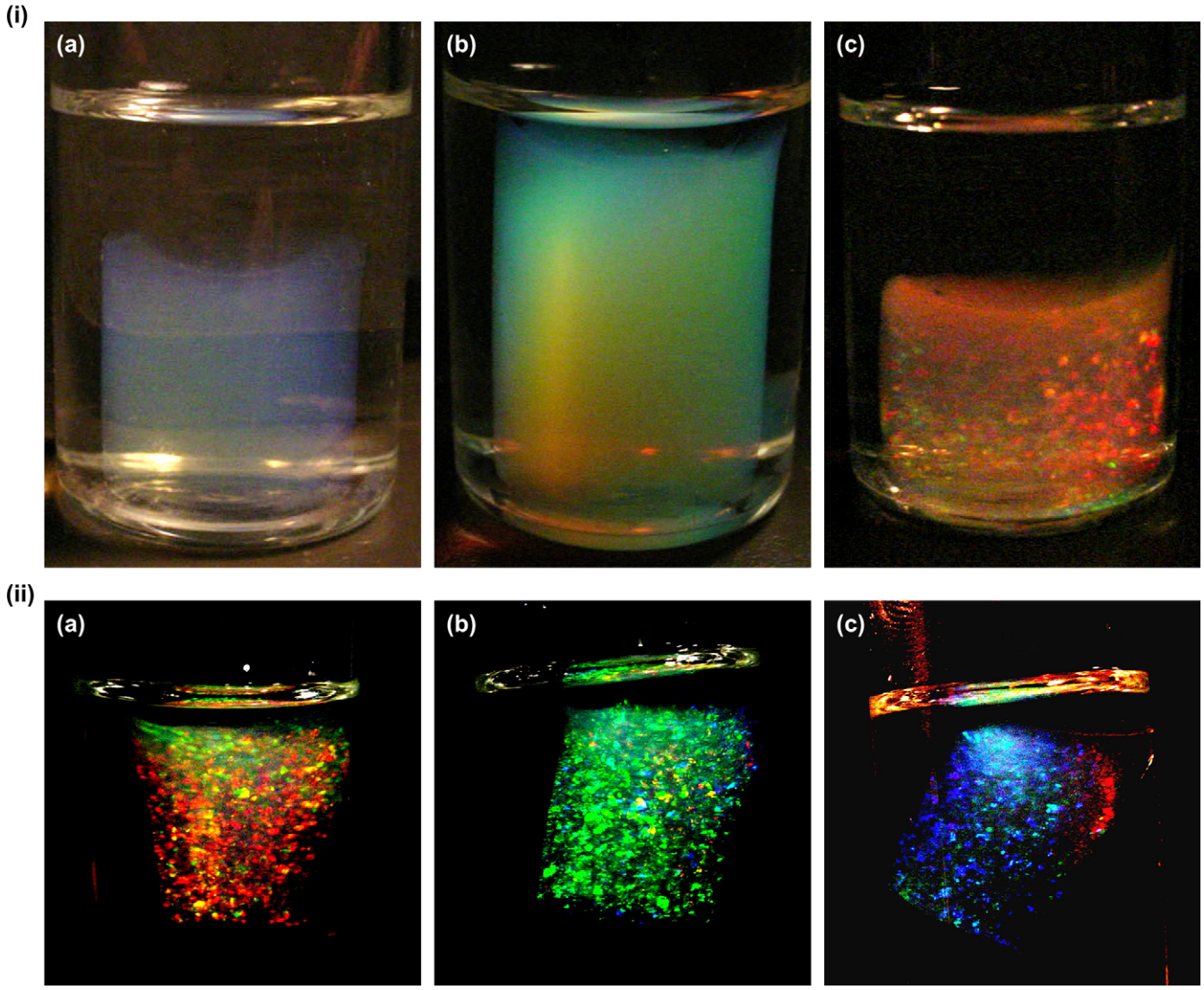

Fig. 3. (i) Crystalline PNIPAM-*co*-AA gels with particle sizes in acetone: Hydrodynamic radii ($\langle R_h \rangle$) of precursor particles in water are (a) 122 nm (blue, Batch I), (b) 161 nm (light green, Batch II), and (c) 213 nm (multi-colors, Batch III), respectively. The solid content is 10 wt%. (ii) Bragg diffraction of crystalline PNIPAM-*co*-AA gel (Batch III) suspended in epichlorohydrin. The color of the gel changes with the scattering angle between the incident beam and the scattered light recorded by a camera. From left to right, (a) 165°, (b) 145° and (c) 85°.

Kinetics of the solvent exchange process was shown in Fig. 4(ii). A critical phase transition point was observed at time around 60 min. The collapse of the crystalline gel at this point is the result of the volume phase transition induced by changing the solvent composition inside the polymer gel. It is the effect of co-nonsolvency that both solvents are good ones but the mixture of them is a poor solvent. The shrinkage of a PNIPAM gel in mixed solvents including water–methanol, water–ethanol, and water–acetic acid has been studied [28]. We have used this effect to precipitate PNIPAM-*co*-AA nanoparticles in water–acetone mixture (~20:80 acetone–water). When an acetone swollen PNIPAM-*co*-AA gel nanoparticle network was placed in a large quantity of water, the whole process of replacement of solvent from acetone to water took several hours, leading to the solvent composition changing from pure acetone to a mixture of acetone and water, and eventually to pure water. The shrinking process follows an exponential decay with an average decay time of ~3 min; the subsequent swelling process is an exponential growth process with an average growth time of ~250 min. The swelling speed depends on the elastic force from macroscopic view and on the affinity between polymer chain network and solvent molecules from microscopic view. The remnant acetone inside the gel, though the concentration is low, may partially destroy the hydrogen bond between gel and water, which is the major driven force for gel to swell, and that may explain the slow swelling kinetics.

The crystalline gel shows good resilient property even after solvent exchange from acetone to water (Fig. 5(i)). When an external force was applied perpendicular to the surface of the gel, as shown in Fig. 5(i)-b, the crystals temporarily disappeared because of the gel distortion. After the force was removed, the gel recovered its original form and the crystals appeared again. The recurrence of the crystals further confirms that the

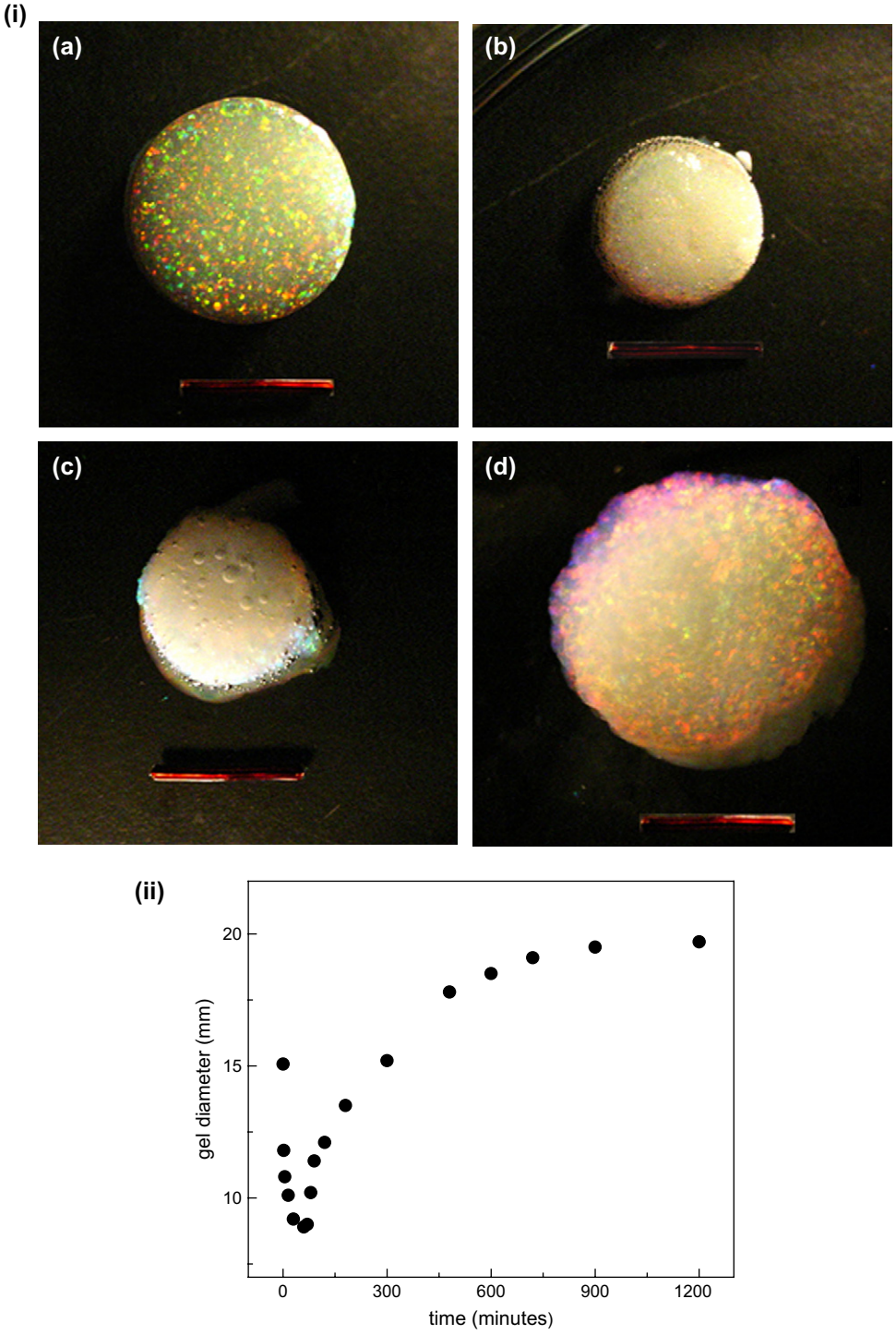

Fig. 4. (i) Solvent exchange (acetone–water) process (Batch III): (a) 0 min, (b) 5 min, (c) 120 min and (d) 900 min. The diameter of cylindrical crystalline PNIPAM-*co*-AA gel is 15 mm at time of zero. The gel was immersed into a glass culture dish with 120 ml water. (ii) The shrinking and swelling kinetics during solvent exchange process. A transition point appears at 60 min.

crystals have been fixed in their positions. This elastomer property of the crystalline gel may have potential applications.

When the volume of the gels is kept constant, the stress–strain response of ideal networks under uniaxial compression or extension is characterized as follows [29]:

$$\tau = F/A_0 = G_0\left(\delta - \delta^{-2}\right) \tag{2}$$

where τ is the engineering stress, F is the applied force, A_0 is the undeformed cross-sectional area of swollen polymers, $G_0 = N_0 k_B T$ is the shear modulus, N_0 is the number of chains per unit volume, k_B is Boltzmann constant, T is the absolute temperature, $\delta = L/L_0$ is the strain, with L sample length under stress, and L_0 undeformed sample length. At low strains, a plot of stress τ versus $(\delta - \delta^{-2})$ yields a straight line whose slope is

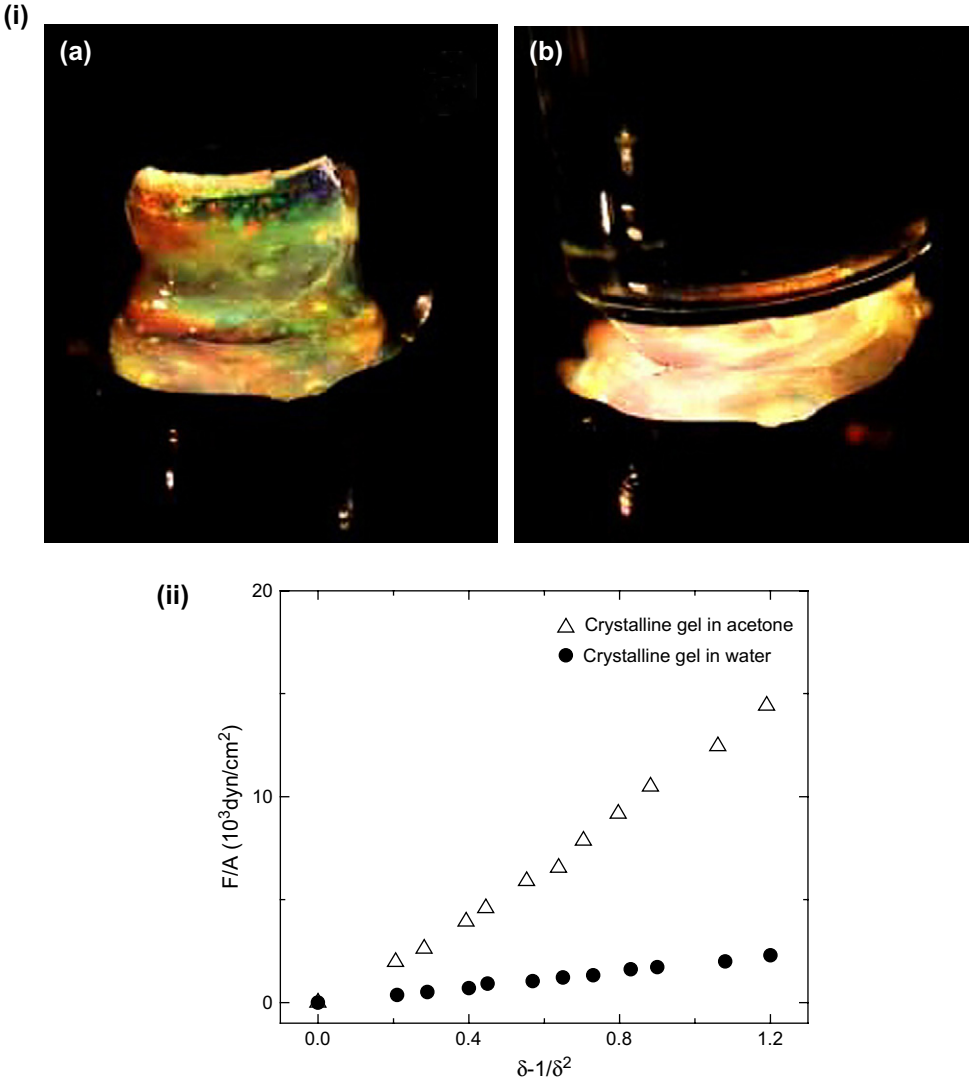

Fig. 5. (i) Elastic test of crystalline gel (Batch III, after solvent exchange) (a) before pressing and (b) after pressing. (ii) Shear modulus (G) measurement of the crystalline PNIPAM-*co*-AA gels (Batch III) in acetone (Δ) ($G_{acetone} = 1.3 \times 10^4$ dyn/cm^2) and in water (●) ($G_{water} = 0.2 \times 10^4$ dyn/cm^2).

the shear modulus G_0. The shear modulus of the crystalline gel before and after solvent exchange was measured, as is shown in Fig. 5(ii). The crystalline gel has higher modulus (1.3×10^4 dyn/cm^2) in acetone than one (0.2×10^4 dyn/cm^2) in water. This is mainly due to the higher crystallization concentration in acetone than that in water.

4. Conclusions

Monodispersed PNIPAM-*co*-AA gel nanoparticles with different particle sizes have been synthesized using precipitation polymerization. The particle sizes were controlled by adding different amounts of surfactant (sodium dodecyl sulfate) in the pre-gel solution. It is found that at polymer concentration about 10 wt%, nanoparticles have not only strong interaction but also enough freedom to form large colloidal crystals in acetone. These crystals are easy to observe due to their iridescent patterns. The decrease in particle size reduces the inter-particle distance so that the color shifts to a shorter wavelength. The carboxyl group on the surface of PNIPAM-*co*-AA nanoparticles can be further cross-linked in acetone by epichlorohydrin at ~90 °C to form three-dimensional nanoparticle network. The resultant gels exhibit different opalescent colors corresponding different particle sizes, governed by Bragg diffraction. Due to their high solid contents, the crystalline gels have good mechanical strength that is essential for materials applications. They can also undergo a solvent exchange from acetone to water without damaging their crystalline structures. Kinetics of the solvent exchange was measured and explained in terms of the volume phase transition of the PNIPAM in mixed solvents. Combining good mechanical properties and unique optical features, crystalline gels may find their applications in sensors, membranes for chemical separation and carriers for controlled drug delivery.

Acknowledgement

We gratefully acknowledge the support from the National Science Foundation under Grant No. DMR-0507208. We

thank Shijun Tang for his assistance in mechanical measurements.

References

[1] (a) Peppas NA. Hydrogels in medicine and pharmacy. Boca Raton, FL: CRC Press; 1987;
(b) Peppas NA, Langer R. Science 1994;263:1715.
[2] Hoffman AS. Artif Organs 1995;19:455.
[3] Siegel RA, Firestone BA. Macromolecules 1988;21:3254.
[4] Kopecek J. Eur J Pharm Sci 2003;20:1.
[5] Osada Y, Gong JP. Adv Mater 1998;10:827.
[6] Akashi R, Tsutsui H, Komura A. Adv Mater 2002;14:1808.
[7] Weissman JM, Sunkara HB, Tse AS, Asher SA. Science 1996;274:959.
[8] Sankara HB, Jethmalani JM, Ford WT. Chem Mater 1994;6:362.
[9] Pan G, Kesavamoorthy R, Asher SA. J Am Chem Soc 1998;120:6525.
[10] Holtz JH, Asher SA. Nature 1997;389:829.
[11] (a) Hu ZB, Lu XH, Gao J, Wang C. Adv Mater 2000;12:1173;
(b) Hu ZB, Lu XH, Gao J. Adv Mater 2001;13:1708.
[12] Lyon LA, Debord JD, Debord SB, Jones CD, McGrath JG, Serpe MJ. J Phys Chem B 2004;108:19099.
[13] Asher SA, Alexeev VL, Goponenko AV, Sharma AC, Lednev IK, Wilcox CS, et al. J Am Chem Soc 2003;125:3322.
[14] (a) Debord JD, Lyon LA. J Phys Chem 2000;104:6327;
(b) Debord JD, Eustis S, Debord SB, Lofye MT, Lyon LA. Adv Mater 2002;14:658.
[15] (a) Takeoka Y, Watanabe M. Langmuir 2002;18:5977;
(b) Takeoka Y, Watanabe M. Adv Mater 2003;15:199.
[16] Lee YJ, Braun PV. Adv Mater 2003;15:563.
[17] Lee YJ, Pruzinsky SA, Braun PV. Langmuir 2004;20:3096.
[18] Tsuji S, Kawaguchi H. Langmuir 2005;21:2434.
[19] Pusey PN, Megan MV. Nature 1986;320:340.
[20] Hu ZB, Huang G. Angew Chem Int Ed 2003;42:4799.
[21] Pelton RH, Chibante P. Colloids Surf 1986;20:247.
[22] Berne BJ, Pecora R. Dynamic light scattering. New York: Wiley; 1976.
[23] Chu B. Laser light scattering. 2nd ed. New York: Academic Press; 1991.
[24] Tanaka T. Sci Am 1981;244:1.
[25] Hirotsu Y, Hirokawa T, Tanaka T. J Chem Phys 1987;87:1392.
[26] Gao J, Frisken BJ. Langmuir 2003;19:5212.
[27] Gao J, Hu ZB. Langmuir 2002;18:1360.
[28] Tanaka T. Phys Rev Lett 1978;40:820.
[29] Gehrke SH. Adv Polym Sci 1993;110:81.